INSTITUTE OF PHYSICS PUBLISHING JOURNAL OF OPTICS B: QUANTUM AND SEMICLASSICAL OPTICS
J. Opt. B: Quantum Semiclass. Opt. **7** (2005) S392–S397 doi:10.1088/1464-4266/7/10/027

Photon subtracted states and enhancement of nonlocality in the presence of noise

Stefano Olivares and Matteo G A Paris

Dipartimento di Fisica and INFM, Università degli Studi di Milano, Italy

E-mail: Stefano.Olivares@mi.infn.it and Matteo.Paris@fisica.unimi.it

Received 25 February 2005, accepted for publication 12 May 2005
Published 26 September 2005
Online at stacks.iop.org/JOptB/7/S392

Abstract
We address nonlocality of bipartite continuous variable systems in the presence of dissipation and noise. Three nonlocality tests have been considered, based on the measurement of displaced parity, field quadrature and pseudospin operator, respectively. Nonlocality of twin-beams has been investigated, as well as that of their non-Gaussian counterparts obtained by inconclusive subtraction of photons. Our results indicate that (i) nonlocality of twin-beams is degraded but not destroyed by noise; (ii) photon subtraction enhances nonlocality in the presence of noise, especially in the low-energy regime.

Keywords: nonlocality, Bell inequalities, entanglement, conditional measurements

1. Introduction

Nonlocality, i.e. the existence of correlations which cannot be explained by any local hidden variable model, is perhaps the most debated implication of quantum mechanics. During the last decade other aspects of nonlocality, in addition to generating nonlocal correlations, have been discovered: for example, the possibility of teleporting and effectively encoding quantum information, as well as the ability to perform certain computations exponentially faster than any classical device.

Realistic implementations of quantum information protocols require the investigation of nonlocality in a noisy environment. In particular, the robustness of nonlocality should be addressed, as well as the design of protocols to preserve and possibly enhance nonlocality in the presence of noise.

The evolution of nonlocality for a twin-beam state of radiation (TWB) in a thermal environment was studied in [1] by means of the displaced parity test [2], whereas in [3] its nonlocality was investigated using the pseudospin operators [4] when only dissipation occurs.

In [5] we have suggested a conditional measurement scheme on TWB leading to a non-Gaussian entangled mixed state, which improves the fidelity of teleportation of coherent states. This process, named inconclusive photon subtraction (IPS), is based on mixing each mode of the TWB with the vacuum in an unbalanced beam splitter and then performing inconclusive photodetection on both modes, i.e. revealing the reflected beams without discriminating the number of detected photons. IPS states have the following properties: they improve the teleportation fidelity for coherent states [5] and show enhanced nonlocal correlations in the phase space [6] in ideal conditions, namely in the absence of noise. Motivated by these results and by the recent experimental generation of IPS states [7], in this paper we extend the previous studies on the TWB and consider the nonlocality of the IPS state in the presence of noise.

The paper is structured as follows. In section 2 we address the evolution of TWBs in a noisy channel where both dissipation and thermal noise are present, whereas in section 3 we briefly review the IPS process. In sections 4, 5 and 6 we investigate the nonlocality of TWB and IPS by means of three different tests: displaced parity, homodyne detection (field-quadrature) and pseudospin test, respectively. Finally, section 7 closes the paper with some concluding remarks.

2. Dynamics of TWB in noisy channels

The so called twin-beam state of radiation (TWB), i.e. $|\Lambda\rangle\rangle = \sqrt{1-\lambda^2}\sum_k \lambda^k |k\rangle \otimes |k\rangle$ with $\lambda = \tanh r$, r being the TWB

squeezing parameter, is usually obtained by parametric down-conversion of the vacuum, $|\Lambda\rangle\rangle = \exp\{r(a^\dagger b^\dagger - ab)\}|0\rangle$, a and b being field operators. It is described by the Gaussian Wigner function

$$W_0(\alpha,\beta) = \frac{\exp\{-2\tilde{A}_0(|\alpha|^2+|\beta|^2)+2\tilde{B}_0(\alpha\beta+\alpha^*\beta^*)\}}{4\pi^2\sqrt{\mathrm{Det}[\boldsymbol{\sigma}_0]}}, \tag{1}$$

with

$$\tilde{A}_0 = \frac{A_0}{16\sqrt{\mathrm{Det}[\boldsymbol{\sigma}_0]}}, \qquad \tilde{B}_0 = \frac{B_0}{16\sqrt{\mathrm{Det}[\boldsymbol{\sigma}_0]}}, \tag{2}$$

where $A_0 \equiv A_0(r) = \cosh(2r)$, $B_0 \equiv B_0(r) = \sinh(2r)$ and $\boldsymbol{\sigma}_0$ is the covariance matrix

$$\boldsymbol{\sigma}_0 = \tfrac{1}{4}\begin{pmatrix} A_0\mathbb{I}_2 & B_0\boldsymbol{\sigma}_3 \\ B_0\boldsymbol{\sigma}_3 & A_0\mathbb{I}_2 \end{pmatrix}, \tag{3}$$

$\mathbb{I}_2$ being the 2×2 identity matrix and $\boldsymbol{\sigma}_3 = \mathrm{Diag}(1,-1)$. Using a more compact form, equation (1) can also be rewritten as

$$W_0(\boldsymbol{X}) = \frac{\exp\{-\frac{1}{2}\boldsymbol{X}^{\mathrm{T}}\boldsymbol{\sigma}_0^{-1}\boldsymbol{X}\}}{4\pi^2\sqrt{\mathrm{Det}[\boldsymbol{\sigma}_0]}}, \tag{4}$$

with $\boldsymbol{X} = (x_1, y_1, x_2, y_2)^{\mathrm{T}}$, $\alpha = x_1 + \mathrm{i}y_1$ and $\beta = x_2 + \mathrm{i}y_2$, and $(\cdots)^{\mathrm{T}}$ denoting the transposition operation.

When the two modes of the TWB interact with a noisy environment, namely in the presence of dissipation and thermal noise, the evolution of the Wigner function (1) is described by the following Fokker–Planck equation [8–10]:

$$\partial_t W_t(\boldsymbol{X}) = \tfrac{1}{2}\big(\partial_{\boldsymbol{X}}^{\mathrm{T}}\mathbb{\Gamma}\boldsymbol{X} + \partial_{\boldsymbol{X}}^{\mathrm{T}}\mathbb{\Gamma}\boldsymbol{\sigma}_\infty\partial_{\boldsymbol{X}}\big)W_t(\boldsymbol{X}), \tag{5}$$

with $\partial_{\boldsymbol{X}} = (\partial_{x_1}, \partial_{y_1}, \partial_{x_2}, \partial_{y_2})^{\mathrm{T}}$. The damping matrix reads $\mathbb{\Gamma} = \bigoplus_{k=1}^{2}\Gamma_k\mathbb{I}_2$, whereas the asymptotic covariance matrix is given by

$$\boldsymbol{\sigma}_\infty = \bigoplus_{k=1}^{2}\boldsymbol{\sigma}_\infty^{(k)} = \begin{pmatrix} \boldsymbol{\sigma}_\infty^{(1)} & \mathbf{0} \\ \mathbf{0} & \boldsymbol{\sigma}_\infty^{(2)} \end{pmatrix}, \tag{6}$$

where $\mathbf{0}$ is the 2×2 null matrix and

$$\boldsymbol{\sigma}_\infty^{(k)} = \tfrac{1}{4}\begin{pmatrix} 1+2N_k & 0 \\ 0 & 1+2N_k \end{pmatrix}. \tag{7}$$

Γ_k, N_k denote the damping rate and the average number of thermal photons of channel k, respectively. $\boldsymbol{\sigma}_\infty$ represents the covariance matrix of the environment and, in turn, the asymptotic covariance matrix of the evolved TWB. Since the environment is itself excited in a Gaussian state, the evolution induced by (5) preserves the Gaussian form (4). The covariance matrix at time t reads as follows [10, 11]:

$$\boldsymbol{\sigma}_t = \mathbb{G}_t^{1/2}\boldsymbol{\sigma}_0\mathbb{G}_t^{1/2} + (\mathbb{I} - \mathbb{G}_t)\boldsymbol{\sigma}_\infty, \tag{8}$$

where $\mathbb{G}_t = \bigoplus_{k=1}^{2}\mathrm{e}^{-\Gamma_k t}\mathbb{I}_2$. The covariance matrix $\boldsymbol{\sigma}_t$ can also be written as

$$\boldsymbol{\sigma}_t = \tfrac{1}{4}\begin{pmatrix} A_t(\Gamma_1,N_1)\mathbb{I}_2 & B_t(\Gamma_1)\boldsymbol{\sigma}_3 \\ B_t(\Gamma_2)\boldsymbol{\sigma}_3 & A_t(\Gamma_2,N_2)\mathbb{I}_2 \end{pmatrix} \tag{9}$$

with

$$\begin{aligned} A_t(\Gamma_k,N_k) &= A_0\mathrm{e}^{-\Gamma_k t} + (1-\mathrm{e}^{-\Gamma_k t})(1+2N_k), \\ B_t(\Gamma_k) &= B_0\mathrm{e}^{-\Gamma_k t}. \end{aligned} \tag{10}$$

Let us now consider channels with the same damping rate Γ but different number of thermal photons, N_1 and N_2: using the density matrix formalism, the state corresponding to the covariance matrix (9) has the following form:

$$\varrho_t = S_2(\xi)\mu_1\otimes\mu_2 S_2^\dagger(\xi), \tag{11}$$

where μ_k is the thermal state

$$\mu_k = \frac{1}{1+M_k}\left(\frac{M_k}{1+M_k}\right)^{a_k^\dagger a_k} \tag{12}$$

a_k, $k=1,2$ being the mode operators. The average numbers of photons are given by

$$M_1 = \tfrac{1}{4}\left[\sqrt{A_+^2 - 16B_t} - (2 - A_-)\right], \tag{13}$$

$$M_2 = \tfrac{1}{4}\left[\sqrt{A_+^2 - 16B_t} - (2 + A_-)\right], \tag{14}$$

$A_\pm = A_{1,t} \pm A_{2,t}$, $A_{k,t} \equiv A_t(\Gamma, N_k)$ and $B_t = B_t(\Gamma)$. In equation (11) $S_2(\xi) = \exp\{\xi a_1^\dagger a_2^\dagger - \xi^* a_1 a_2\}$ denotes the two-mode squeezing operator, with parameter $\xi\in\mathbb{C}$

$$|\xi| = \sinh^{-1}\left(\sqrt{\frac{A_+}{2(A_+^2-16B_t)^{1/2}} - \frac{1}{2}}\right), \tag{15}$$

$$\arg[\xi] = \pi/2. \tag{16}$$

Equation (11) says that the quantum state of a TWB, after propagating in a noisy channel, is the same as a state obtained by parametric down-conversion from a noisy background [11]. Their properties, and in particular entanglement and nonlocality, can be addressed in a unified way using equation (11) or, equivalently, equations (9) and (10).

Finally, if we assume $\Gamma_1 = \Gamma_2 = \Gamma$ and $N_1 = N_2 = N$, then the covariance matrix (9) becomes formally identical to (3) and the corresponding Wigner function reads

$$W_t(\alpha,\beta) = \frac{\exp\{-2\tilde{A}_t(|\alpha|^2+|\beta|^2)+2\tilde{B}_t(\alpha\beta+\alpha^*\beta^*)\}}{4\pi^2\sqrt{\mathrm{Det}[\boldsymbol{\sigma}_t]}}, \tag{17}$$

with

$$\tilde{A}_t = \frac{A_t(\Gamma,N)}{16\sqrt{\mathrm{Det}[\boldsymbol{\sigma}_t]}}, \qquad \tilde{B}_t = \frac{B_t(\Gamma)}{16\sqrt{\mathrm{Det}[\boldsymbol{\sigma}_t]}}, \tag{18}$$

whereas the density matrix, *mutatis mutandis*, is still given by equation (11).

3. De-Gaussification and noise

When thermal noise and dissipation affect the propagation of an entangled state, its nonlocal properties are reduced and, finally, destroyed [9, 10, 12]. Therefore, it is of interest to look for some technique in order to preserve, at least in part, such correlations, or to enhance the nonlocality of the state which will face the lossy transmission line. Since it has been shown that the de-Gaussification of a TWB can enhance its entanglement in the ideal case and since non-Gaussian states can be produced using the current technology [7], in this and the following sections we will investigate whether or not this process can also be useful in the presence of noise.

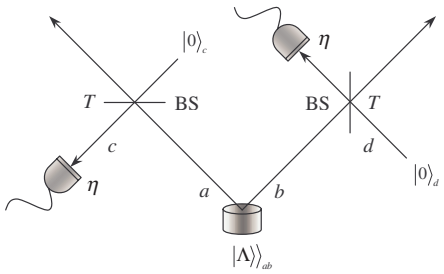

Figure 1. Scheme of the IPS process: the two modes of a bipartite state $|\Lambda\rangle_{ab}$ are mixed with the vacuum at two unbalanced beam splitters (BSs) and the reflected modes are revealed by avalanche photodetectors (APDs) with quantum efficiency η. When the APDs jointly click one has the IPS state.

(This figure is in colour only in the electronic version)

The de-Gaussification of a TWB can be achieved by subtracting photons from both modes [5, 13, 14]. In [5] we referred to this process as inconclusive photon subtraction (IPS) and showed that the resulting state, the IPS state, can be used to enhance the teleportation fidelity of coherent states for a wide range of the experimental parameters. Moreover, in [6], we have shown that, in the absence of any noise during the transmission stage, the IPS state has nonlocal correlations larger than those of the TWB irrespective of the IPS quantum efficiency (see also [15, 16]).

First of all we briefly recall the IPS process, whose scheme is sketched in figure 1. The two modes, a and b, of the TWB are mixed with the vacuum (modes c and d, respectively) at two unbalanced beam splitters (BSs) with equal transmissivities; the modes c and d are then revealed by avalanche photodetectors (APDs) with equal efficiencies, which can only discriminate the presence of radiation from the vacuum: the IPS state is obtained when the two detectors jointly click. The mixing with the vacuum at a beam splitter with transmissivity T followed by the on/off detection with quantum efficiency η is equivalent to mixing with an effective transmissivity τ [5]

$$\tau \equiv \tau(T, \eta) = 1 - \eta(1 - T), \tag{19}$$

followed by an ideal (i.e. efficiency equal to 1) on/off detection. Using the Wigner formalism, when the input state arriving at the two beam splitters is the TWB $W_0(\alpha, \beta)$ of equation (1), the state produced by the IPS process reads as follows (see [6] for the details about the calculation and about the de-Gaussification map for the density matrix and Wigner function in the case of a TWB):

$$W_0^{(\mathrm{IPS})}(\alpha, \beta) = \frac{1}{\pi^2 p_{11}(r, \tau)} \sum_{k=1}^{4} \mathcal{C}_k(r, \tau) W_{r,\tau}^{(k)}(\alpha, \beta), \tag{20}$$

where

$$p_{11}(r, \tau) = \sum_{k=1}^{4} \frac{\mathcal{C}_k(r, \tau)}{(b - f_k)(b - g_k) - (2\tilde{B}_0\tau + h_k)^2} \tag{21}$$

is the probability of a click in both the APDs. In equations (20) and (21) we introduced

$$W_{r,\tau}^{(k)}(\alpha, \beta) = \exp\{-(b - f_k)|\alpha|^2 - (b - g_k)|\beta|^2 + (2\tilde{B}_0\tau + h_k)(\alpha\beta + \alpha^*\beta^*)\}, \tag{22}$$

and defined

$$\mathcal{C}_k(r, \tau) = \frac{C_k}{\sqrt{\mathrm{Det}[\boldsymbol{\sigma}_0]}[x_k y_k - 4\tilde{B}_0^2(1 - \tau)^2]}, \tag{23}$$

where $C_1 = 1$, $C_2 = C_3 = -2$, $C_4 = 4$; $x_k \equiv x_k(r, \tau)$, and $y_k \equiv y_k(r, \tau)$ are given by

$$x_1 = x_3 = y_1 = y_1 = a$$

$$x_2 = x_4 = y_3 = y_4 = a + 2$$

with $a \equiv a(r, \tau) = 2[\tilde{A}_0(1 - \tau) + \tau]$, $b \equiv b(r, \tau) = 2[\tilde{A}_0\tau + (1 - \tau)]$. Finally, f_k, g_k, and h_k depend on r and τ as follows

$$f_k = \mathcal{N}_k[x_k\tilde{B}_0^2 + 4\tilde{B}_0^2(1 - \tilde{A}_0)(1 - \tau) + y_k(1 - \tilde{A}_0)^2], \tag{24}$$

$$g_k = \mathcal{N}_k[x_k(1 - \tilde{A}_0)^2 + 4\tilde{B}_0^2(1 - \tilde{A}_0)(1 - \tau) + y_k\tilde{B}_0^2], \tag{25}$$

$$h_k = \mathcal{N}_k\{(x_k + y_k)\tilde{B}_0(1 - \tilde{A}_0) + 2\tilde{B}_0[\tilde{B}_0^2 + (1 - \tilde{A}_0)^2](1 - \tau)\}, \tag{26}$$

$$\mathcal{N}_k \equiv \mathcal{N}_k(r, \tau) = \frac{4\tau(1 - \tau)}{x_k y_k - 4\tilde{B}_0^2(1 - \tau)^2}. \tag{27}$$

The state corresponding to equation (20) is no longer a Gaussian state and its nonlocal properties, in ideal conditions, were studied in [6].

Here we are interested in the case when the IPS process is performed on a TWB evolved in a noisy environment with both the channels having the same damping rate and thermal noise. The Wigner function of the state arriving at the beam splitters is now given by equation (17), and the output state is still described by equation (20), but with the following substitutions:

$$\tilde{A}_0 \to \tilde{A}_t, \qquad \tilde{B}_0 \to \tilde{B}_t, \qquad \boldsymbol{\sigma}_0 \to \boldsymbol{\sigma}_t. \tag{28}$$

We will denote with $W_{\Gamma,N}^{(\mathrm{IPS})}(\alpha, \beta)$ the Wigner function of this degraded IPS state.

In the next sections we will analyse the nonlocality of the IPS state in the presence of noise by means of the CHSH version of Bell's inequalities for three different kinds of measurement.

4. Nonlocality in the phase space

Parity is a dichotomic variable and thus can be used to establish Bell-like inequalities [17]. The displaced parity operator for two modes is defined as [2]

$$\hat{\Pi}(\alpha, \beta) = D_a(\alpha)(-1)^{a^\dagger a} D_a^\dagger(\alpha) \otimes D_b(\beta)(-1)^{b^\dagger b} D_b^\dagger(\beta), \tag{29}$$

where $\alpha, \beta \in \mathbb{C}$, a and b are mode operators and $D_a(\alpha) = \exp\{\alpha a^\dagger - \alpha^* a\}$ and $D_b(\beta)$ are single-mode displacement operators. Since the two-mode Wigner function $W(\alpha, \beta)$ can be expressed as [11]

$$W(\alpha, \beta) = \frac{4}{\pi^2}\Pi(\alpha, \beta), \tag{30}$$

$\Pi(\alpha, \beta)$ being the expectation value of $\hat{\Pi}(\alpha, \beta)$, the nonlocality revealed through measurement of $\hat{\Pi}(\alpha, \beta)$ is also known as nonlocality in the phase space. The quantity involved

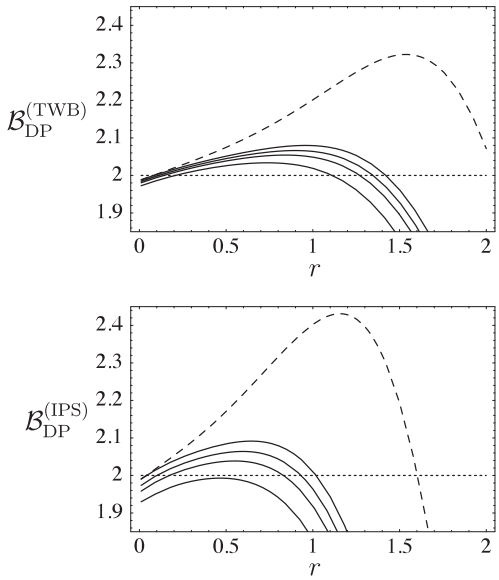

Figure 2. Plots of the Bell parameters $\mathcal{B}_{\rm DP}$ for the TWB (top) and IPS (bottom); we set $\mathcal{J} = 1.6 \times 10^{-3}$ and $\tau = 0.9999$. The dashed lines refer to the absence of noise ($\Gamma t = N = 0$), whereas, for both the plots, the solid lines are $\mathcal{B}_{\rm DP}$ with $\Gamma t = 0.01$ and, from top to bottom, $N = 0, 0.05, 0.1$, and 0.2. In the ideal case the maxima are $\mathcal{B}_{\rm DP}^{\rm (TWB)} = 2.32$ and $\mathcal{B}_{\rm DP}^{\rm (IPS)} = 2.43$, respectively.

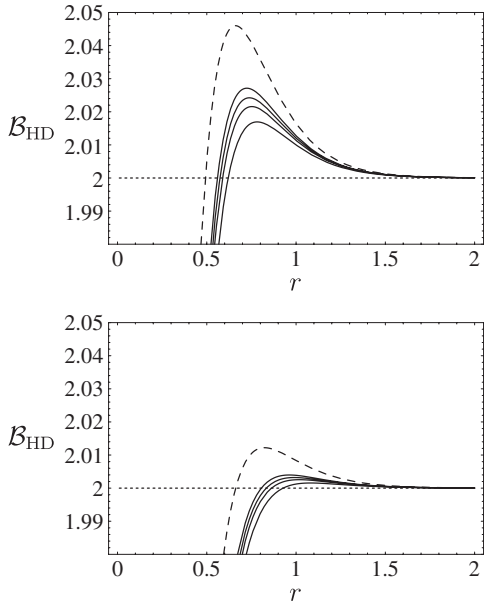

Figure 3. Plots of the Bell parameter $\mathcal{B}_{\rm HD}$ for the IPS states for two different values of the homodyne detection efficiency: $\eta_{\rm H} = 1$ (top), and $\eta_{\rm H} = 0.9$ (bottom). We set $\tau = 0.99$. The dashed lines refer to the absence of noise ($\Gamma t = N = 0$), whereas, for both the plots, the solid lines are $\mathcal{B}_{\rm HD}$ with $\Gamma t = 0.05$ and, from top to bottom, $N = 0, 0.05, 0.1$ and 0.2.

in such inequalities, named the Bell parameter, can be written as follows:

$$\mathcal{B}_{\rm DP} = \Pi(\alpha_1, \beta_1) + \Pi(\alpha_2, \beta_1) + \Pi(\alpha_1, \beta_2) - \Pi(\alpha_2, \beta_2), \quad (31)$$

which, for local theories, satisfies $|\mathcal{B}_{\rm DP}| \leqslant 2$.

Following [2], one can choose a particular set of displaced parity operators, arriving at the following combination [6]:

$$\mathcal{B}_{\rm DP}(\mathcal{J}) = \Pi(\sqrt{\mathcal{J}}, -\sqrt{\mathcal{J}}) + \Pi(-3\sqrt{\mathcal{J}}, -\sqrt{\mathcal{J}}) + \Pi(\sqrt{\mathcal{J}}, 3\sqrt{\mathcal{J}}) - \Pi(-3\sqrt{\mathcal{J}}, 3\sqrt{\mathcal{J}}), \quad (32)$$

which, for the TWB, gives a maximum $\mathcal{B}_{\rm DP} = 2.32$, greater than the value 2.19 obtained in [2]. Notice that, even in the infinite squeezing limit, the violation is never maximal, i.e. $|\mathcal{B}_{\rm DP}| < 2\sqrt{2}$ [18].

In [6] we studied equation (32) for both the TWB and the IPS state in an ideal scenario, namely in the absence of dissipation and noise; we showed that, using IPS, the maximum violation is achieved for $\tau \to 1$ and for values of r smaller than for the TWB.

Now, by means of equation (20) and substitutions (28), we can study how noise affects $\mathcal{B}_{\rm DP}$. The results are shown in figure 2: as one may expect, the overall effect of noise is to reduce the violation of the Bell inequality. When dissipation alone is present ($N = 0$), the maximum of violation is achieved using the IPS for values of r smaller than for the TWB, as in the ideal case. On the other hand, one can see that the presence of thermal noise mainly affects the IPS results. In fact, for $\Gamma t = 0.01$ and $N = 0.2$, one has $|\mathcal{B}_{\rm DP}^{\rm (TWB)}| > 2$ for a range of r values, whereas $|\mathcal{B}_{\rm DP}^{\rm (IPS)}|$ falls below the threshold for violation.

We conclude that, considering the displaced parity test in the presence of noise, the IPS is quite robust if the thermal noise is below a threshold value (depending on the environmental parameters) and for small values of the TWB parameter r.

5. Nonlocality and homodyne detection

In principle there are two approaches to test the Bell inequalities for the bipartite state: either one can employ some test for continuous variable systems, such as that described in section 4, or one can convert the problem to Bell's inequality tests on two qubits by mapping the two modes into two-qubit systems. In this and the following section we will consider this latter case.

The Wigner function $W_0^{\rm (IPS)}(\alpha, \beta)$ given in equation (20) is no longer positive-definite and thus it can be used to test the violation of Bell's inequalities by means of homodyne detection, i.e. measuring the quadratures x_ϑ and x_φ of the two IPS modes a and b, respectively, as proposed in [15, 16]. In this case, one can dichotomize the measured quadratures assuming as outcome +1 when $x \geqslant 0$, and −1 otherwise. The nonlocality of $W_0^{\rm (IPS)}(\alpha, \beta)$ in ideal conditions has been studied in [6], where we also discussed the effect of the homodyne detection efficiency $\eta_{\rm H}$.

Let us now focus our attention on $W_{\Gamma,N}^{\rm (IPS)}(\alpha, \beta)$, namely the state produced when the IPS process is applied to the TWB evolved through the noisy channel. After the dichotomization of the homodyne outputs, one obtains the following Bell parameter:

$$\mathcal{B}_{\rm HD} = E(\vartheta_1, \varphi_1) + E(\vartheta_1, \varphi_2) + E(\vartheta_2, \varphi_1) - E(\vartheta_2, \varphi_2), \quad (33)$$

where ϑ_k and φ_k are the phases of the two homodyne measurements at modes a and b, respectively, and

$$E(\vartheta_h, \varphi_k) = \int_{\mathbb{R}^2} {\rm d}x_{\vartheta_h}\, {\rm d}x_{\varphi_k}\, {\rm sgn}[x_{\vartheta_h}\, x_{\varphi_k}]\, P(x_{\vartheta_h}, x_{\varphi_k}), \quad (34)$$

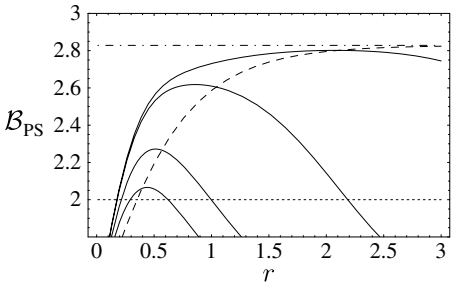

Figure 4. Plots of the Bell parameter $\mathcal{B}_{\rm PS}$ in the ideal case ($\Gamma t = N = 0$): the dashed line refers to the TWB, whereas the solid lines refer to the IPS with, from top to bottom, $\tau = 0.9999, 0.99, 0.9$ and 0.8. There is a threshold value for r below which IPS gives a higher violation than TWB. Note that there is also a region of small values of r for which the IPS state violates the Bell inequality while the TWB does not. The dash–dotted line is the maximal violation value $2\sqrt{2}$.

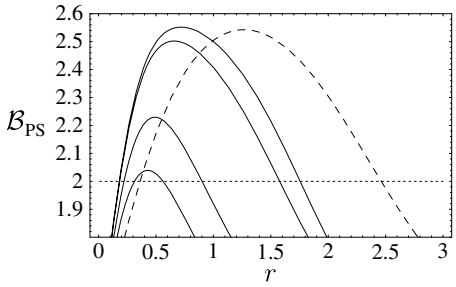

Figure 5. Plots of the Bell parameter $\mathcal{B}_{\rm PS}$ for $\Gamma t = 0.01$: the dashed line refers to the TWB, whereas the solid lines refer to the IPS with, from top to bottom, $\tau = 0.9999, 0.99, 0.9$ and 0.8. The same comments as in figure 4 still hold.

$P(x_{\vartheta_h}, x_{\varphi_k})$ being the joint probability of obtaining the two outcomes x_{ϑ_h} and x_{φ_k} [16]. As usual, violation of Bell's inequality is achieved when $|\mathcal{B}_{\rm HD}| > 2$.

In figure 3 we plot $\mathcal{B}_{\rm HD}$ for $\vartheta_1 = 0$, $\vartheta_2 = \pi/2$, $\varphi_1 = -\pi/4$ and $\varphi_2 = \pi/4$: as for the ideal case [6, 16], the Bell inequality is violated for a suitable choice of the squeezing parameter r. Obviously, the presence of noise reduces the violation, but we can see that the effect of thermal noise is not so large as in the case of the displaced parity test addressed in section 4 (see figure 2).

Notice that the high efficiencies of this kind of detectors allow a loophole-free test of hidden variable theories [19], though the violations obtained are quite small. This is due to the intrinsic information loss of the binning process, which is used to convert the continuous homodyne data in dichotomic results [20].

6. Nonlocality and pseudospin test

Another way to map a two-mode continuous variable system into a two-qubit system is by means of the pseudospin test: this consists in measuring three single-mode Hermitian operators S_k satisfying the Pauli matrix algebra $[S_h, S_k] = 2\mathrm{i}\varepsilon_{hkl}S_l$, $S_k^2 = \mathbb{I}$, $h, k, l = 1, 2, 3$, and ε_{hkl} is the totally antisymmetric tensor with $\varepsilon_{123} = +1$ [3, 4]. For the sake of clarity, we will refer to S_1, S_2 and S_3 as S_x, S_y and S_z, respectively. In this way one can write the following correlation function:

$$E(\mathbf{a}, \mathbf{b}) = \langle (\mathbf{a}\cdot\mathbf{S})(\mathbf{b}\cdot\mathbf{S})\rangle, \tag{35}$$

where $\mathbf{a}$ and $\mathbf{b}$ are unit vectors such that

$$\begin{aligned} \mathbf{a}\cdot\mathbf{S} &= \cos\vartheta_a S_z + \sin\vartheta_a(\mathrm{e}^{\mathrm{i}\varphi_a}S_- + \mathrm{e}^{-\mathrm{i}\varphi_a}S_+), \\ \mathbf{b}\cdot\mathbf{S} &= \cos\vartheta_b S_z + \sin\vartheta_b(\mathrm{e}^{\mathrm{i}\varphi_b}S_- + \mathrm{e}^{-\mathrm{i}\varphi_b}S_+), \end{aligned} \tag{36}$$

with $S_\pm = \frac{1}{2}(S_x \pm \mathrm{i}S_y)$. In the following, without loss of generality, we set $\varphi_k = 0$. Finally, the Bell parameter reads

$$\mathcal{B}_{\rm PS} = E(\mathbf{a}_1, \mathbf{b}_1) + E(\mathbf{a}_1, \mathbf{b}_2) + E(\mathbf{a}_2, \mathbf{b}_1) - E(\mathbf{a}_2, \mathbf{b}_2), \tag{37}$$

corresponding to the CHSH Bell inequality $|\mathcal{B}_{\rm PS}| \leqslant 2$. In order to study equation (37) we should choose a specific representation of the pseudospin operators; note that, as pointed out in [21, 22], the violation of Bell inequalities for continuous variable systems depends on, besides the orientational parameters, the chosen representation, since different S_k leads to different expectation values of $\mathcal{B}_{\rm PS}$. Here we consider the pseudospin operators corresponding to the Wigner functions [21]

$$W_x(\alpha) = \frac{1}{\pi}\,\mathrm{sgn}\big[\mathrm{Re}[\alpha]\big], \qquad W_z(\alpha) = -\tfrac{1}{2}\delta^{(2)}(\alpha), \tag{38}$$

$$W_y(\alpha) = -\frac{1}{2\pi}\delta\big(\mathrm{Re}[\alpha]\big)\mathcal{P}\frac{1}{\mathrm{Im}[\alpha]}, \tag{39}$$

where $\mathcal{P}$ denotes the Cauchy principal value. Thanks to (38) one obtains

$$\begin{aligned} E_{\rm TWB}(\mathbf{a}, \mathbf{b}) &= \cos\vartheta_a\cos\vartheta_b \\ &+ \frac{2\sin\vartheta_a\sin\vartheta_b}{\pi}\arctan\big[\sinh(2r)\big], \end{aligned} \tag{40}$$

for the TWB, and for the IPS

$$\begin{aligned} E_{\rm IPS}(\mathbf{a}, \mathbf{b}) = \sum_{k=1}^{4}\frac{\mathcal{C}_k(r,\tau)}{p_{11}(r,\tau)}\Bigg[&\frac{\cos\vartheta_a\cos\vartheta_b}{4} \\ &+ \frac{2\sin\vartheta_a\sin\vartheta_b}{\pi\mathcal{A}_k}\arctan\left(\frac{2\tilde{B}_0\tau + h_k}{\sqrt{\mathcal{A}_k}}\right)\Bigg] \end{aligned} \tag{41}$$

where $\mathcal{A}_k = (b - f_k)(b - g_k) - (2\tilde{B}_0\tau + h_k)^2$, and all the other quantities have been defined in section 3.

In figure 4 we plot $\mathcal{B}_{\rm PS}$ for the TWB and IPS in the ideal case, namely in the absence of dissipation and thermal noise. For all the figures we set $\vartheta_{a_1} = 0$, $\vartheta_{a_2} = \pi/2$, and $\vartheta_{b_1} = -\vartheta_{b_2} = \pi/4$. As usual, the IPS leads to better results for small values of r. Whereas $\mathcal{B}_{\rm PS}^{(\rm TWB)} \to 2\sqrt{2}$ as $r \to \infty$, $\mathcal{B}_{\rm PS}^{(\rm IPS)}$ has a maximum and then falls below the threshold of two as r increases. It is interesting to note that there is a region of small values of r for which $\mathcal{B}_{\rm PS}^{(\rm TWB)} \leqslant 2 < \mathcal{B}_{\rm PS}^{(\rm IPS)}$, i.e. the IPS process can increase the nonlocal properties of a TWB which does not violate the Bell inequality for the pseudospin test in such a way that the resulting state violates it. This fact is also present in the case of the displaced parity test described in section 4, but using the pseudospin test the effect is enhanced. Notice that the maximum violations for the IPS occur for an experimentally achievable range of values of r.

In figure 5 we consider the presence of the dissipation alone and vary τ. We can see that IPS is effective also when the

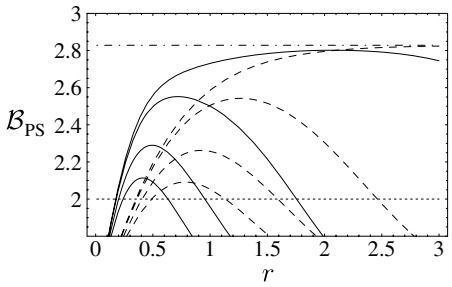

Figure 6. Plots of the Bell parameter $\mathcal{B}_{\rm PS}$ for different values of Γt and in the absence of thermal noise ($N = 0$): the dashed lines refer to the TWB, whereas the solid ones refer to the IPS with $\tau = 0.9999$; for both the TWB and IPS we set, from top to bottom, $\Gamma t = 0, 0.01, 0.05$ and 0.1. The dash–dotted line is the maximal violation value $2\sqrt{2}$.

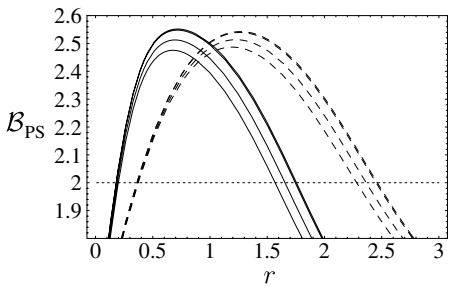

Figure 7. Plots of the Bell parameter $\mathcal{B}_{\rm PS}$ for $\Gamma t = 0.01$ and different values of N: the dashed lines refer to the TWB, whereas the solid ones refer to the IPS with $\tau = 0.9999$; for both the TWB and IPS we set, from top to bottom, $N = 0, 0.01, 0.1$ and 0.2.

effective transmissivity τ is not very high. We take into account the effect of dissipation and thermal noise in figures 6 and 7: we can conclude that IPS is quite robust with respect to these sources of noise and, moreover, one can think of employing IPS as a useful resource in order to reduce the effect of noise.

7. Concluding remarks

We have addressed three different nonlocality tests, namely, displaced parity, homodyne detection and pseudospin tests, on TWBs and IPS states in the presence of noise. We have shown that the IPS process on TWBs enhances nonlocality both in ideal cases and also when noise (dissipation and thermal noise) affects the propagation. As in the ideal situation, the enhancement is achieved when the TWB energy is not too high (small squeezing parameter r), the threshold being dependent on the environmental parameters. Moreover, in the case of the pseudospin test, we have seen that there is a region of small r for which the TWB itself does not violate the Bell inequality, whereas after the IPS process it does.

We conclude that the enhanced nonlocality in the presence of noise makes the IPS states a useful resource for continuous variable quantum information processing.

Acknowledgments

Stimulating and useful discussions with M S Kim, A Ferraro and A R Rossi are gratefully acknowledged. This work is partially supported by MIUR through the project FIRB RBAU014CLC_002.

References

[1] Jeong H, Lee J and Kim M S 2000 *Phys. Rev.* A **61** 052101
[2] Banaszek K and Wódkiewicz K 1998 *Phys. Rev.* A **58** 4345
[3] Filip R and Mista L 2002 *Phys. Rev.* A **66** 044309
[4] Chen Z-B, Pan J-W, Hou G and Zhang Y-D 2002 *Phys. Rev. Lett.* **88** 040406
[5] Olivares S, Paris M G A and Bonifacio R 2003 *Phys. Rev.* A **67** 032314
[6] Olivares S and Paris M G A 2004 *Phys. Rev.* A **70** 032112
[7] Wenger J, Tualle-Bouri R and Grangier P 2004 *Phys. Rev. Lett.* **92** 153601
[8] Walls D and Milburn G 1994 *Quantum Optics* (Berlin: Springer)
[9] Olivares S and Paris M G A 2004 *J. Opt. B: Quantum Semiclass. Opt.* **6** 69
[10] Serafini A, Illuminati F, Paris M G A and De Siena S 2004 *Phys. Rev.* A **69** 023318
[11] Ferraro A, Olivares S and Paris M G A 2005 *Gaussian States in Quantum Information* (Napoli: Bibliopolis)
[12] Rossi A R, Olivares S and Paris M G A 2004 *J. Mod. Opt.* **51** 1057
[13] Opatrný T, Kurizki G and Welsch D-G 2000 *Phys. Rev.* A **61** 032302
[14] Cochrane P T, Ralph T C and Milburn G J 2002 *Phys. Rev.* A **65** 062306
[15] Nha H and Carmichael H J 2004 *Phys. Rev. Lett.* **93** 020401
[16] García-Patrón Sánchez R *et al* 2004 *Phys. Rev. Lett.* **93** 120409
García-Patrón R, Fiurášek J and Cerf N J 2005 *Phys. Rev.* A **71** 022105
[17] Clauser J F, Horne M A, Shimony A and Holt R A 1969 *Phys. Rev. Lett.* **23** 880
[18] Jeong H *et al* 2003 *Phys. Rev.* A **67** 012106
[19] Gilchrist A, Deuar P and Reid M D 1998 *Phys. Rev. Lett.* **80** 3169
Gilchrist A, Deuar P and Reid M D 1999 *Phys. Rev.* A **60** 4259
[20] Munro W J 1999 *Phys. Rev.* A **59** 4197
[21] Gour G *et al* 2003 *Phys. Lett.* A **324** 415
Revzen M *et al* 2005 *Phys. Rev.* A **71** 022103
[22] Ferraro A and Paris M G A 2005 *J. Opt. B: Quantum Semiclass. Opt.* **7** 174